EverRing: Powering Battery-Free, Highly-Capable Smart Rings with Headset RF Energy

Nathan DeVrio
Carnegie Mellon University
Pittsburgh, PA, USA
ndevrio@cmu.edu

Chris Harrison
Carnegie Mellon University
Pittsburgh, PA, USA
chris.harrison@cs.cmu.edu

Figure 1: We developed EverRing, a smart ring that has no battery and never needs to be recharged. Instead, we use an RF transmitter incorporated into an XR headset/glasses (A), which is less battery- and space-constrained than a ring, to wirelessly power our ring (B). With less need to conserve power to extend runtime, our ring (C) offers a rich suite of input and output capabilities. For instance, as an XR accessory, it could provide eyes-free interface navigation using its directional tactile switch, use its IMU to aid in low-power hand tracking, and even provide haptic feedback when interacting with virtual widgets — capabilities not presently offered by any other smart ring, chiefly due to limited battery power.

Abstract

Rings are a powerful form factor for interaction in XR. Being located on a finger and near other digits, they are well positioned to enable rich human-computer input and outputs, such as micro-gesture sensing and providing haptic feedback. Compared to other wearables, such as watches and earbuds, rings are less obtrusive, so much so that some users wear them continuously. However, their small size inherently means small batteries, and thus very limited I/O capabilities. This led us to ask: how can we create a ring that does not need to be removed to be recharged, and has sufficient power to continuously support rich interactions? This led us to develop EverRing, a battery-less ring device powered wirelessly by RF energy transmitted from an XR headset (and future glassses). In evaluations, we quantify how much RF power can be captured wirelessly in the interactive volume in front of a user, how much power each input and output capability consumes, and how the ring maintains a balanced power budget in common XR use cases (productivity, gaming, etc.).

CCS Concepts

• **Human-centered computing** → **Interaction devices**.

This work is licensed under a Creative Commons Attribution 4.0 International License.
ISWC '25, Espoo, Finland
© 2025 Copyright held by the owner/author(s).
ACM ISBN 979-8-4007-1481-8/2025/10
https://doi.org/10.1145/3715071.3750420

Keywords

Smart Ring; Battery-Free; Mixed Reality; Wearable; Input

ACM Reference Format:
Nathan DeVrio and Chris Harrison. 2025. EverRing: Powering Battery-Free, Highly-Capable Smart Rings with Headset RF Energy. In *Proceedings of the 2025 ACM International Symposium on Wearable Computers (ISWC '25), October 12–16, 2025, Espoo, Finland*. ACM, New York, NY, USA, 8 pages. https://doi.org/10.1145/3715071.3750420

1 Introduction

Smart rings are an increasingly popular category of wearable devices. Wearing rings is already deeply ingrained in many cultures, and by being worn on the hand, rings are excellently positioned to track active input from the fingers and passively sense hand interactions. Our goal in this work is to better realize the full potential of smart rings as highly-capable input and output accessories.

We note that current smart rings have a major inherent limitation: due to their small and slim form factor, they can only include very small batteries, often on the order of 20-30 mAh. Small batteries force hardware designers into a significant tradeoff: either a short runtime with rich capabilities, or reduce capabilities to extend runtime. Commercial smart ring offerings have chosen the latter avenue. For example, the Oura smart ring [13] has to be charged roughly once per week, but only offers very-low-duty-cycle physiological sensing. On the other hand, research-oriented ring projects tend to focus on one advanced capability, but are either tethered to power or use a battery that only lasts a few hours [3, 9, 11, 17, 18].

In response to these limitations, we considered a novel approach to power smart rings. Our explorations culminated in EverRing, a prototype ring device that requires no charging and has no battery at all. Instead, EverRing receives power via RF energy transmitted wirelessly from a worn headset/glasses into the space in front of the user where interactions generally occur. This energy is used to power a capable microcontroller (MCU) with a rich array of input and output capabilities, including Bluetooth communication. We envision EverRing as an input accessory, worn and used in conjunction with XR headsets or glasses (which offer rich output capabilities, but tend to be input bottlenecked).

We note that previous work has enabled battery-free passive sensing [43], or wirelessly powered active sensing, but only for short ranges (e.g., from the wrist to the fingers [44]) or using much larger transmitter hardware (e.g., torso-sized inductive coils [45]). Our approach is both compact (able to be integrated into an XR headset) and far-field (sufficient power even at an arm's length).

2 Literature Review

In this section we summarize research on low-power and battery-free wearables with properties relevant to EverRing. Organizing by property, we first discuss different energy harvesting techniques used by battery-free wearables. We conclude with techniques for body-scale wireless power transmission.

2.1 Energy-Harvesting Wearables

For wearable devices, batteries are often seen as a hindrance because they increase bulk and need to be recharged. For this reason, many prior works have attempted to create wearables that can operate with very small batteries, or even no battery at all, and instead harvest energy from their surroundings. In contrast to wireless power transmission techniques, these systems collect energy passively and do not require an external device to emit energy.

Many different techniques have been utilized for energy harvesting, including solar [48], RF [34, 48], movement of the user's body [46, 53], and even perspiration [15]. For RF, common ambient sources to harvest include WiFi, 5G, and Bluetooth [5]. The energy available to harvest from ambient wireless signals is minuscule (nanowatts at room scale) [2], which is a reason why we did not explore it for this project.

Another class of systems that use an active transmitter, but themselves act purely passively, are battery-free RFID systems such as WISP [40]. These systems, including wearable variants [16], work by receiving an RFID signal and using its energy to briefly power sensors or a microcontroller that change the properties of the backscattered signal. The transmitter looks for changes in the reflected signal to measure a change in sensor value on the battery-free device [16, 40].

2.2 Body-Scale Wireless Power Transmission

An alternative to passively harvesting sources of ambient energy is to receive energy from an external device that is actively transmitting. This technique is more commonly known as wireless power transmission (WPT) and is the technique that we use in our system.

Many different mechanisms have been explored for enabling body-scale WPT. Some examples include inductive coils [26, 43–45, 54], magnetic resonance [21], electrode coupling [55], body coupling [19, 20, 22, 32, 38, 52], ultrasound [33], laser [42], NFC [6, 10, 23], and RF [8, 25, 37, 39, 47, 50]. Of these, the most popular tend to be inductive coils, body coupling, and RF (which we use).

Inductive coils have the main advantage of a very high efficiency (up to ~80%) [43]. The downside is that this high efficiency is attained only at a very short ranges (a few centimeters) [43]. We attempted a ring-sized coil for an early prototype, but found the range to be far too short (<5-10 cm) to be powered from a headset transmitter. Range can be extended using larger or additional transmitting coils, potentially integrated into clothing as seen in Takahashi et al. [45].

Another approach are "body coupled" systems that send a very small amount of current at high frequency through the user's epidermal tissue [19, 20, 22, 38]. While body-scale ranges can be achieved, the main downside is received power is low, especially at longer distances such as head to hand (158 μW in [19]).

Wireless RF power offers a balanced approach. Unlike inductive coils, RF can achieve much longer ranges, and compared to body coupling, received power at the hand is greater (300-800 μW) [24, 49]. One of the downsides of RF is that similar to inductive coils, transmission efficiency is greatly improved when the size or shape of the receiver (in this case an antenna) is increased. Prior works with high efficiency use large antennas infeasible for a wearable [49]; smaller antennas are far less efficient [27]. As such, a great deal of research has focused specifically on how to optimize antenna designs to best receive power when worn on the body [34, 39, 50], which we also explored and discuss.

3 Implementation

In this section we detail our proof-of-concept EverRing prototype. We begin by discussing how our wireless power transmission works, then discuss the design of our antenna and physical ring. Next, we provide details on the embedded system, including hardware and software components. We then offer a power consumption analysis of each of the input/output capabilities we selected for inclusion in our prototype. We conclude with discussion of how these hardware capabilities could support rich interaction use cases.

3.1 Wireless Power Transmission

The goal of our system is to obviate the need for a battery, which we do by transmitting power wirelessly through the air using RF waves. To do this, we use an RF transmitter mounted at a slight downward angle on a Meta Quest 3 headset [28] (Figure 1A) and an antenna on our ring (Figure 1C). In this setup, power is taken from the battery of the headset and used to power the transmitter. The energy is captured by the ring's antenna and stored in a supercapacitor on the ring for present or future use.

For an RF transmitter, we selected the PowerCast TX91503 [36]. This is a standalone module, powered with a USB cable, that emits 915 MHz RF. The transmitter is a rectangular PCB patch antenna and measures 14.4 × 2.0 cm. In a future design, we imagine this antenna would be integrated directly into the front of the headset, or the front frame of a pair of XR glasses.

Figure 2: Photos of our final proof-of-concept ring.

Power transmission at 915 MHz has been successfully demonstrated in the past [37, 47]. Beyond the proven advantages of this style of wireless power transmission, we chose PowerCast's module primarily for its compact size, and, together with the Quest 3, for their ease of setup, and availability. Nevertheless, the principles we present are also valid for alternative headsets and transmitters.

When operating, the TX91503 transmits 3.0 W Effective Isotropic Radiated Power (EIRP) in its normal direction and consumes 4.0 W of power (from the headset battery in our case). This level of power transmission has been certified by the FCC to be safe for use around humans, although care should be taken for individuals with pacemakers or at higher risk [36]. Since the PowerCast module beams power broadly, multiple antennas could receive power at the same time (e.g., multiple EverRings, or other wearables).

3.2 Antenna Design

To receive the power emanating from our transmitter, we first designed and constructed a custom antenna for our ring. When designing this antenna, we had to consider several challenges. For one, users expect that a smart ring should be compact and unobtrusive, thus our antenna cannot extend too far out from the finger. On the other hand, due to the conductive properties of human tissue, antennas in close proximity to the skin are significantly attenuated [1, 29]. These two challenges come directly into conflict because a worn antenna performs better when it is larger or placed further from the body [1], however doing this directly contributes to bulk.

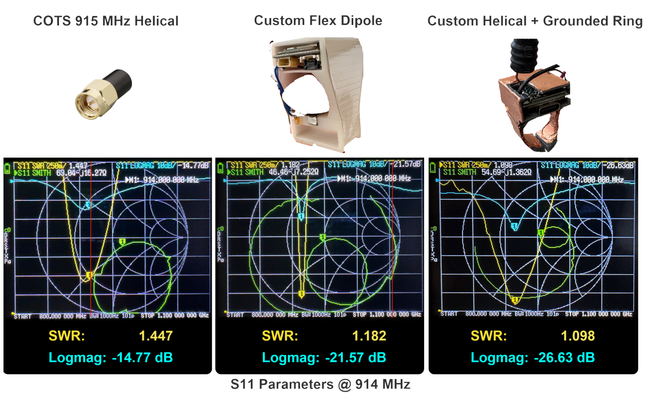

Figure 3: VNA measurements comparing the performance of the three antennas we tested during our prototyping process. Of the three, our final custom helical and body grounded ring antenna achieved the best overall performance.

Considering these constraints, we made a flexible PCB antenna design with a long length that meandered to optimize performance at 915 MHz, while remaining compact (Figure 3, center). To counteract the body attenuation issue, we designed the feed point of the antenna to be as close as possible to the finger and the receiving end to be as far away as possible. While we found our custom antenna performed better than a commercial off-the-shelf 915 MHz monopole antenna (Figure 3, left), our design was also much more sensitive to orientation, which is problematic for a ring that can be in many different 3D orientations relative to the headset as the hand moves. In addition, we found this design was strongly affected by closeness to the finger, with performance being significantly better when worn on the tip of the finger rather than below the second knuckle like a typical ring.

For our next antenna design iteration (Figure 3, right), we took advantage of the monopole antenna's omnidirectional radiation pattern, while improving performance near the finger. This was accomplished by making a helical monopole with a large ground plane on the entire outside of the ring to maximize conductive skin contact with the finger. This design was inspired by theory for wearable antennas that dictates attenuation can be minimized by increasing the size of the ground pole of the antenna and minimizing the potential difference between the antenna ground and the skin [29]. Performance can still vary with ring orientation, but the effect is minor as it is uncomfortable to pitch the finger in the direction aligned with the antenna's null axis (perpendicular to top of ring).

Figure 3 shows plots contrasting performance of the three antennas we explored. Standing wave ratio (SWR) is a common antenna metric used to measure how much power is transmitted from a source to a load. S11 is an SWR measurement indicating how much of the signal entering an antenna is reflected back due to impedance mismatch. A higher number (further from zero) indicates less reflection and better antenna performance. At a tuned frequency of 914 MHz, our final design attained a S11 SWR of 1.1, which is 7% better than our first design (flexible PCB antenna) and 24% better than a commercial monopole antenna.

3.3 Physical Ring Design

A photo of our prototype ring is shown in Figure 2. Unlike many existing smart rings, which distribute their volume equally about the circumference of the finger, we opted for a form factor more akin to sports championship ring. This shape moves the bulk of the components to the top of the ring, while minimizing volume on the sides. The benefit of this design, beyond comfort, is to maximize the distance between the antenna and skin, reducing attenuation (a key finding from the prior section). Beyond the antenna, the inner volume of the ring is filled with the remaining components, including our MCU, supercapacitors, sensors, haptic actuator, etc.

3.4 Embedded Hardware

We created our own embedded hardware to collect, store, and manage power, provide compute, and control sensors. The custom PCB that we designed is shown in Figure 4, which mates to a nRF52840 microcontroller (we use a modified XIAO board) [41]. Our PCB

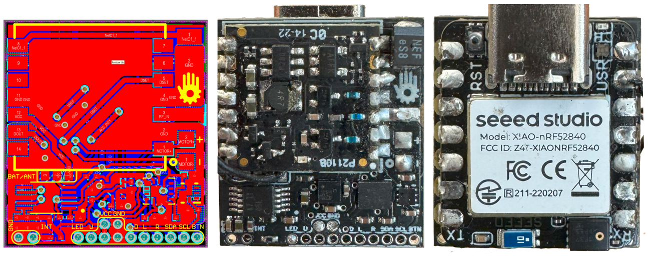

Figure 4: Design and layout of our sensing and control PCB.

also accommodates a PowerCast P2110B RF-to-DC daughter board [35]. We specifically chose the nRF52 platform due to its low-power modes and built-in Bluetooth Low Energy (BLE) communication stack. In typical operation, we keep our microcontroller in an ultra-low power sleep mode and wake it up using timer interrupts or trigger interrupts from sensors to know when to collect a new sensor value and send it over BLE.

Our PCB directly hosts, or is wired to an array of input / output components: an infrared LED, time-of-flight (ToF) depth sensor, five-way tactile switch (four directions + click), haptic actuator (LRA), accelerometer, and magnetometer. These components are shown and summarized in Figures 1, 5 and 6. We discuss how different combinations of these input and output capabilities can power interactive uses cases in Section 4.

3.5 Power Consumption

A breakdown of the power consumption and test conditions of each of our system's interactive features can be found in Figure 6. A major takeaway from our power analysis was the large disparity in power consumption between different components that enable similar interactive capabilities. For example, the five-way tactile switch consumed only 1 μW for directional input, while the accelerometer consumed 216 μW (at 25 Hz) for 3D pointing. For a number of basic interactions, such as navigating a menu interface, both input techniques enable a similar set of controls, however one consumes two orders more energy. In addition, many of the components have multiple data rates or interrupt modes modes that drastically change how much power is consumed. As such, depending on the power available, designers may choose to tradeoff higher framerate sensing for more reliable operation or the use of more sensors.

4 Example Interactive Uses

We curated a set of input/output capabilities for our prototype ring to highlight the potential of our approach. To convey this, we provide a series of example use cases our ring can support, which have been previously explored in the literature. We note the set of sensors and inputs we selected is not definitive or exhaustive, and future rings could include a different mix of components to support other useful interactions. At a high level, our guiding ethos was to maximize the number of interactions for the lowest power cost.

Directional Input - Directional input is one of the most foundational ways to interact with a user interface. We considered a number of different components, including a hall-effect joystick, a trackball, a potentiometer-based joystick, and a five-way tactile switch (up/down/left/right/click). Of these, we selected the latter because it not only consumed little to no power when not in use, but also could use its discrete switch changes to trigger interrupts to wake the microcontroller from sleep.

Clicks & Taps - Also foundational for input is the ability to confirm an input or action with a click or tap. In our system, there are two ways to achieve this. At an extremely low power cost, clicks can be performed with the center function of our five-way tactile switch. As an alternative, we also have a BMI270 3-axis accelerometer [4] that can detect sharp spikes in acceleration corresponding to taps of the finger. To enable this, the accelerometer can be programmed either in a polling (higher power, more data for other uses) or interrupt (lowest power) mode.

3D Pointing - In cases with a larger number of selectable elements, directional input may be too slow. Instead, it may be preferable to point a ray in 3D space to make a selection. In fact, "point and click" interaction is perhaps the most valuable interaction missing from many contemporary smart glasses. By fusing data from our ring's accelerometer and magnetometer [30], we generate an estimate of the 3D orientation of the ring finger, which can be used for pointing.

Hand Tracking - Hand tracking for input in XR headsets and glasses is currently achieved with cameras and deep learning models, both of which are power-expensive. As one alternative, we can use our ring's infrared LED, which can be readily segmented from the background with basic (and low-power) heuristics. We note that current XR headsets, including the Meta Quest 3S and Apple Vision Pro already contain monochrome cameras sensitive to infrared light, and could be used for stereo tracking of an IR LED. Similar to other sensors, the LED does not have to run continuously and can be pulsed to save power at the cost of less frequent updates.

Fingertip Micro-Gestures - Depending on the use context and application, some users may prefer to perform more subtle finger micro-gestures. For this, we included a VL53L1 time-of-flight (ToF) depth sensor [31] on the bottom of our ring, enabling mid-air thumb gestures. Thumb swipes to the side of the index finger are also possible if the sensor is located on the side of the ring.

Held Object Detection - As XR headsets and glasses become more capable with the integration of AI agents, they will also have increased capabilities to adapt to the user's context. For example, a headset is normally asleep to save power and protect privacy, but our ring could detect when the user picks up an object and the headset/glasses could take a picture to find out what it is and if the user needs contextual assistance. In this example, our ring can use the ToF sensor in an interrupt mode (which is much lower power than the polling mode; see Figure 6) to detect when there is an object abutting the ring in the user's palm.

Haptic Feedback - Finally, beyond input, a smart ring could also have the ability to provide output information to its wearer. We integrated a VLV041235L linear resonant actuator (LRA) [51] powered by a DRV2605L motor driver [14] to provide haptic feedback. Though the most power-hungry component in our system, we believe that haptic feedback can offer great value. For instance, it could provide haptic feedback when clicking a virtual button in XR. We note, however, that even in optimal conditions (ring operating

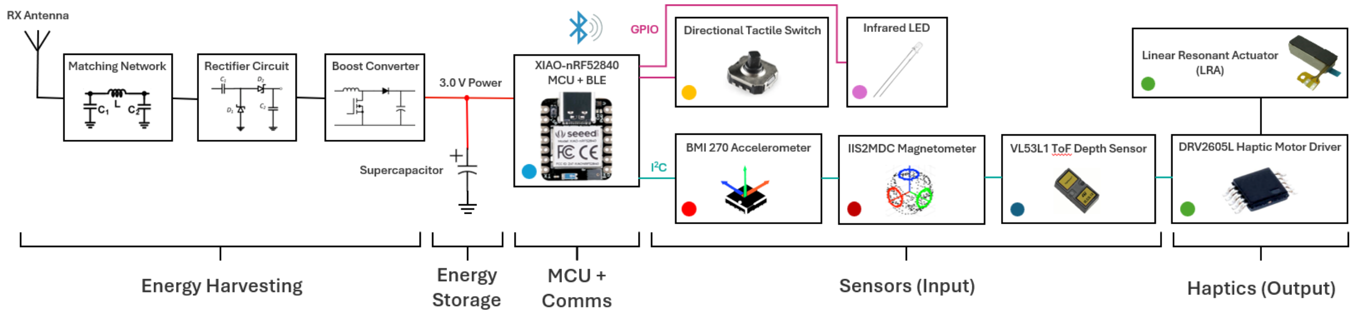

Figure 5: Complete diagram outlining the components of EverRing. Received RF energy passes through energy harvesting circuitry to convert it to DC power which is stored for later use. Using this energy, our MCU can be programmed based on the application to control various input sensor and output haptics while communicating to external devices.

Component	Mode	Average power (μW)
5-way tactile switch	Continuous	1
BMI270 3-axis accelerometer	10 Hz 25 Hz	102 216
IIS2MDC 3-axis magnetometer	10 Hz	83
IR LED	Continuous	1098
VL53L1 ToF depth sensor	1 Hz 10 Hz 20 Hz	1500 4350 7800
DRV2605L haptic LRA driver	Standby 35 ms pulse, 30% peak ampl., 1 Hz 35 ms pulse, 100% peak ampl., 1 Hz 43 ms pulse, 100% peak ampl., 1 Hz	9 2100 6060 8550
nRF52 microcontroller	Standby BLE TX: 32 byte packet, 1 Hz BLE TX: 32 byte packet, 25 Hz	16 32 231

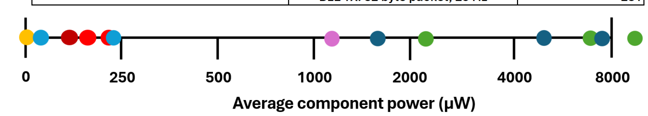

Figure 6: Table detailed the power consumption of each of our system's components in various operating modes. Below the table we plot (on a log scale) the average power of components for easier comparison.

directly in front of the user at 25 cm), our ring can only harvest enough power for a short haptic event roughly once a second. Of course, our ring can accumulate charge in its supercapacitor, which if fully charged, has enough power for approximately 400 haptic events. However, our ring does not have, nor can harvest, enough power for e.g., haptic feedback when continuously typing.

5 Evaluation

To evaluate how well EverRing performed at capturing transmitted wireless power, we conducted a user evaluation. The goal of the study was to collect measurements of harvested power for the entire region or "cloud" of possible positions the ring might inhabit in front of the user (and thus headset) during typical XR use. For this study we recruited 10 participants (5 male, 5 female, mean age 25.5). The study lasted 25 minutes, was conducted in a typical office space, and participants were compensated $10. After completing consent paperwork, participants wore a Quest 3 headset instrumented with the RF transmitter and our ring on their right index finger.

We made one small modification to our hardware to capture accurate readings of harvested power. Specifically, instead of connecting the output of the energy harvesting circuit to the supercapacitor and MCU, we connected it directly to a shunt resistor and powered the MCU off of a LiPo battery. The MCU took measurements every 10 ms (100 FPS) of the shunt current using its 10-bit ADC and transmitted the result to a laptop over BLE. On the laptop, we ran a custom Unity program which used the Quest 3 hand tracking API to log the 3D position of the ring relative to the headset.

During the study, we rendered outlines of floating shapes in front of the user in XR that periodically scaled, rotated, and translated within specified ranges. We prompted users to use the outlines as paths and follow them with the ring. The goal was to generate broad coverage of the tracking area in front of the headset. Every 30 seconds the path changed to a new shape (square, circle, triangle, star, figure-eight, repeat). After 10 minutes, participants were given a break, then the orientation of the shapes was changed from horizontal to vertical and the task repeated. In total 1.2 million power measurements were collected (10 participants × 20 min × 100 FPS).

6 Results & Discussion

In this section we share findings from our evaluation and implications of those findings for application developers and practitioners.

6.1 Received Power

The results from our power measurement study are visualized in Figure 7. To generate these "power clouds", we aggregated the measurements from all participants into a single point cloud, then voxelized the point cloud using a voxel size of 1.5 cm. To compute the power value for a voxel, we took the average of all measurements within that voxel. To generate the side, front, and top views in Figure 7, we created 2D projections by taking the max voxel value from each slice along the corresponding axis for that view. Analyzing the voxel clouds, the results mostly matched our expectations given the angle and radiation pattern of our headset transmitter [36]. This is most readily seen in the side view, where a strong cone of received power is projected down and out from the headset (and where the arms would typically inhabit for many XR interactions).

The most interesting pattern was in the top view, where we observed a triangular cone radiating out about 25 cm from the headset, then sharply dropping off with two lobes off to each side. We do not have an exact explanation for this behavior, but we did notice participants tended to change the orientation of their finger

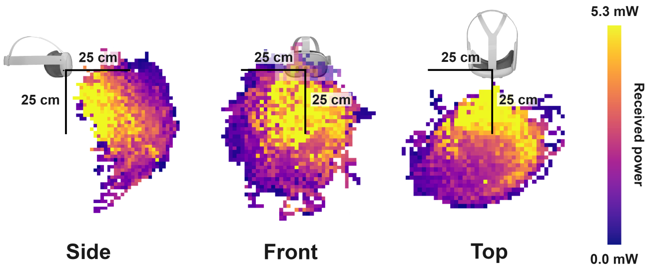

Figure 7: Plots of the voxelized "power clouds" we measured during our user evaluation. Even at an arms length away (30-50 cm), received power is still sufficient to continuously power most of our interactions.

depending on how far away they were reaching. Our RX helical antenna, although omnidirectional, has null regions at its poles. One hypothesis is that when participants reach out further, they also pitched their finger up more, bringing the RX antenna's null axis more in line with the transmitter. This could explain a drop off in received power that happened more rapidly than the gradual fall off with distance, observed in the side and front views.

Finally, considering absolute power values, we were satisfied with performance. When holding their hand at a comfortable arm's length away, the ring still received a respectable ~1.7 mW of power. This amount is much higher than competitive approaches using body coupling [19, 22, 38]. In addition, although not enough to continuously run power-hungry components like the haptic LRA, it is more than sufficient to keep the MCU transmitting regular BLE packets with data from the other sensors, or to charge the supercapacitor and provide infrequent haptic feedback. When the hands are operating closer to the headset, even down by the abdomen, received power is closer to ~3.5 mW, which could enable even power-hungry haptic events at around 1 Hz.

6.2 Implications for Practitioners

We note that our "power clouds" could act as a look-up table of sorts for application designers, mapping 3D coordinates to received power. For instance, if a developer knows where a user might interact with their application (in mid-air, on a table, on a wall, at the waist, etc.), they can utilize our results to get an approximation of received power. A power budget with sensor/actuator duty cycles can then be created. If hand movement is involved developers could collect data on the location of the fingertip over time while using their app, then map and integrate the data to determine the approximate power harvested by EverRing during that activity.

We piloted this method ourselves, collecting one minute of hand tracking data for each of the following activities: *typing at a desk*, *interacting with a mid-air virtual UI*, *playing a VR game (Beat Saber [7])*, and *walking* with hands swaying at our side. Using our power cloud as a look-up table, integrating power received over time, we found in one minute we could harvest 769 joules while typing, 651 joules with a mid-air UI, 648 joules while playing Beat Saber, and 656 joules while walking. These simple examples show how our results have practical utility to help developers estimate how much power could be available to EverRing in their application, and thus what budget they have to spend on ring interactions.

7 Limitations & Future Work

While EverRing makes progress in elevating the capability of smart rings while functionally sidestepping the issue of limited battery capacity, it nevertheless presents tradeoffs in its design and areas for future work we would like to discuss.

First, while we have demonstrated the ability to power a smart ring wirelessly at range, this power is not free and does place an increased burden on the XR headset battery. The battery on the Quest 3 has a 18.88 Wh rating and battery life during games and MR applications averages ~2 hours (9.44 W consumption) [28]. While operating, our transmitter consumes 4.0 W. Thus, we can expect battery life to effectively decrease by 30%. This is an obvious tradeoff for many applications, but this also represents the "worst case" with no significant optimizations. For example, when the ring is close to full charge, or when it is too far from the headset to receive much power, the transmitter could be turned off to save battery.

A second, related limitation is the efficiency of our wireless power transmission. At arm's length, our efficiency was ~0.1% (including RF-to-DC conversion), which is very low. While much less than near-field coil-based techniques [43], our efficiency is on par with other far-field techniques that have attempted wireless power transmission with a similar setup, range, and antenna size [27]. One avenue for improving efficiency is further refinement of the RX antenna design, however there are limits with near-body coupling. A more promising avenue, which could provide huge potential improvement, is the ability to use the tracked location of the ring to beamform [12] RF energy. Directing power only to the ring would greatly reduce excess power radiating into the environment.

Finally, while we made efforts to make our prototype compact, there is still room for improvement. Compared to typically worn jewelry, our ring prototype is bulky. One way to reduce size would be to use a flexible PCB wrapping around the ring body and a redesign of the RX antenna closer to our meandering dipole prototype (Figure 3, center). However, as we noted, there are tradeoffs with received power the closer the antenna is to the skin.

8 Conclusion

We presented our work on EverRing, a novel ring device that never needs to be taken off to charge. EverRing receives its power through the air from an RF transmitter on a paired XR headset via a specialized RX antenna inside the ring. Our ring is highly capable and enables many different interactions including directional input, point and click, micro-gestures, haptic notifications, and more. We provide details on the power consumption of all interactive components in different operating modes and ran a user study to measure received power during typical use. Together, we hope these results can be used in the future by practitioners of our system to design interactive apps that match their anticipated power budget.

Acknowledgments

We thank PowerCast and Charlie Greene, Hank Gasbarro, and Alan Neves for help in developing and utilizing their hardware. We also thank Istvan Szini for his invaluable guidance on antenna design.

References

[1] Usman Ali, Sadiq Ullah, Babar Kamal, Ladislau Matekovits, and Amir Altaf. 2023. Design, Analysis and Applications of Wearable Antennas: A Review. *IEEE Access* 11 (2023), 14458–14486. https://doi.org/10.1109/ACCESS.2023.3243292

[2] Fernando Angulo, Loraine Navarro, Christian G. Quintero M., and Mauricio Pardo. 2021. A Simple WiFi Harvester with a Switching-Based Power Management Scheme to Collect Energy from Ordinary Routers. *Electronics* 10, 10 (Jan. 2021), 1191. https://doi.org/10.3390/electronics10101191 Number: 10 Publisher: Multidisciplinary Digital Publishing Institute.

[3] Roger Boldu, Alexandru Dancu, Denys J.C. Matthies, Thisum Buddhika, Shamane Siriwardhana, and Suranga Nanayakkara. 2018. FingerReader2.0: Designing and Evaluating a Wearable Finger-Worn Camera to Assist People with Visual Impairments while Shopping. *Proceedings of the ACM on Interactive, Mobile, Wearable and Ubiquitous Technologies* 2, 3 (Sept. 2018), 1–19. https://doi.org/10.1145/3264904

[4] Bosch. 2019. Inertial Measurement Unit BMI270. https://www.bosch-sensortec.com/products/motion-sensors/imus/bmi270/

[5] Yung-Wey Chong, Widad Ismail, Kwangman Ko, and Chen-Yi Lee. 2019. Energy Harvesting For Wearable Devices: A Review. *IEEE Sensors Journal* 19, 20 (Oct. 2019), 9047–9062. https://doi.org/10.1109/JSEN.2019.2925638

[6] Christine Dierk, Molly Jane Pearce Nicholas, and Eric Paulos. 2018. AlterWear: Battery-Free Wearable Displays for Opportunistic Interactions. In *Proceedings of the 2018 CHI Conference on Human Factors in Computing Systems*. ACM, Montreal QC Canada, 1–11. https://doi.org/10.1145/3173574.3173794

[7] Beat Games. 2018. Beat Saber - VR rhythm game. https://beatsaber.com/

[8] Mingyuan Gao, Bowen Wang, Ye Yao, Mahdiar Taheri, Ping Wang, Dewei Chu, and Yuerui Lu. 2023. Wearable and long-range MXene 5G antenna energy harvester. *Applied Physics Reviews* 10, 3 (Sept. 2023), 031415. https://doi.org/10.1063/5.0146976

[9] Jun Gong, Yang Zhang, Xia Zhou, and Xing-Dong Yang. 2017. Pyro: Thumb-Tip Gesture Recognition Using Pyroelectric Infrared Sensing. In *Proceedings of the 30th Annual ACM Symposium on User Interface Software and Technology*. ACM, Québec City QC Canada, 553–563. https://doi.org/10.1145/3126594.3126615

[10] Jeremy Gummeson, Bodhi Priyantha, and Jie Liu. 2014. An energy harvesting wearable ring platform for gestureinput on surfaces. In *Proceedings of the 12th annual international conference on Mobile systems, applications, and services*. ACM, Bretton Woods New Hampshire USA, 162–175. https://doi.org/10.1145/2594368.2594389

[11] Aakar Gupta, Cheng Ji, Hui-Shyong Yeo, Aaron Quigley, and Daniel Vogel. 2019. RotoSwype: Word-Gesture Typing using a Ring. In *Proceedings of the 2019 CHI Conference on Human Factors in Computing Systems*. ACM, Glasgow Scotland Uk, 1–12. https://doi.org/10.1145/3290605.3300244

[12] Ali Hajimiri, Behrooz Abiri, Florian Bohn, Matan Gal-Katziri, and Mohith H. Manohara. 2021. Dynamic Focusing of Large Arrays for Wireless Power Transfer and Beyond. *IEEE Journal of Solid-State Circuits* 56, 7 (July 2021), 2077–2101. https://doi.org/10.1109/JSSC.2020.3036895

[13] Oura Health. 2024. Oura Ring. Smart Ring for Fitness, Stress, Sleep & Health. https://ouraring.com

[14] Texas Instruments. 2018. DRV2605L data sheet, product information and support | TI.com. https://www.ti.com/product/DRV2605L

[15] Wenzhao Jia, Gabriela Valdés-Ramírez, Amay J. Bandodkar, Joshua R. Windmiller, and Joseph Wang. 2013. Epidermal Biofuel Cells: Energy Harvesting from Human Perspiration. *Angewandte Chemie International Edition* 52, 28 (2013), 7233–7236. https://doi.org/10.1002/anie.201302922 _eprint: https://onlinelibrary.wiley.com/doi/pdf/10.1002/anie.201302922.

[16] Keiko Katsuragawa, Ju Wang, Ziyang Shan, Ningshan Ouyang, Omid Abari, and Daniel Vogel. 2019. Tip-Tap: Battery-free Discrete 2D Fingertip Input. In *Proceedings of the 32nd Annual ACM Symposium on User Interface Software and Technology*. ACM, New Orleans LA USA, 1045–1057. https://doi.org/10.1145/3332165.3347907

[17] Wolf Kienzle and Ken Hinckley. 2014. LightRing: always-available 2D input on any surface. In *Proceedings of the 27th annual ACM symposium on User interface software and technology*. ACM, Honolulu Hawaii USA, 157–160. https://doi.org/10.1145/2642918.2647376

[18] Maruchi Kim, Antonio Glenn, Bandhav Veluri, Yunseo Lee, Eyoel Gebre, Aditya Bagaria, Shwetak Patel, and Shyamnath Gollakota. 2024. IRIS: Wireless ring for vision-based smart home interaction. In *Proceedings of the 37th Annual ACM Symposium on User Interface Software and Technology*. ACM, Pittsburgh PA USA, 1–16. https://doi.org/10.1145/3654777.3676327

[19] Andy Kong, Daehwa Kim, and Chris Harrison. 2024. Power-over-Skin: Full-Body Wearables Powered By Intra-Body RF Energy. In *Proceedings of the 37th Annual ACM Symposium on User Interface Software and Technology (UIST '24)*. Association for Computing Machinery, New York, NY, USA, 1–13. https://doi.org/10.1145/3654777.3676394

[20] Michinari Kono, Hiromi Nakamura, and Jun Rekimoto. 2017. Intentiō: power distribution through a potentialized human body. In *Proceedings of the 8th Augmented Human International Conference*. ACM, Silicon Valley California USA, 1–10. https://doi.org/10.1145/3041164.3041175

[21] André Kurs, Aristeidis Karalis, Robert Moffatt, J. D. Joannopoulos, Peter Fisher, and Marin Soljačić. 2007. Wireless Power Transfer via Strongly Coupled Magnetic Resonances. *Science* 317, 5834 (July 2007), 83–86. https://doi.org/10.1126/science.1143254 Publisher: American Association for the Advancement of Science.

[22] Jiamin Li, Yilong Dong, Jeong Hoan Park, and Jerald Yoo. 2021. Body-coupled power transmission and energy harvesting. *Nature Electronics* 4, 7 (July 2021), 530–538. https://doi.org/10.1038/s41928-021-00592-y Publisher: Nature Publishing Group.

[23] Rongzhou Lin, Han-Joon Kim, Sippanat Achavananthadith, Selman A. Kurt, Shawn C. C. Tan, Haicheng Yao, Benjamin C. K. Tee, Jason K. W. Lee, and John S. Ho. 2020. Wireless battery-free body sensor networks using near-field-enabled clothing. *Nature Communications* 11, 1 (Jan. 2020), 444. https://doi.org/10.1038/s41467-020-14311-2 Publisher: Nature Publishing Group.

[24] Zhu Liu, Pengde Wu, and Gaosheng Li. 2022. A Multibeam and Surface Plasmonic Clothing With RF Energy-Localized Harvester for Powering Battery-Free Wireless Sensor. *IEEE Internet of Things Journal* 9, 15 (Aug. 2022), 13955–13964. https://doi.org/10.1109/JIOT.2022.3142781

[25] Maho Matsukura, Ryoma Moro, Naoki Keicho, Kohei Shimamura, and Shigeru Yokota. 2022. Wireless Charging for Hovering-Drone via Millimeter Wave. In *2022 Wireless Power Week (WPW)*. IEEE, Bordeaux, France, 772–775. https://doi.org/10.1109/WPW54272.2022.9901342

[26] Alex Mazursky, Aryan Gupta, Andre De La Cruz, and Pedro Lopes. 2025. Power-on-Touch: Powering Actuators, Sensors, and Devices during Interaction. In *Proceedings of the 2025 CHI Conference on Human Factors in Computing Systems*. ACM, Yokohama Japan, 1–16. https://doi.org/10.1145/3706598.3713987

[27] Louis Meile, Anja Ulrich, and Michele Magno. 2019. Wireless Power Transmission Powering Miniaturized Low Power IoT devices: A Revie. 312–317. https://doi.org/10.1109/IWASI.2019.8791433

[28] Meta. 2023. Product Information Sheet Meta Quest 3 | Meta Quest | Meta Store. https://www.meta.com/legal/quest/product-information-sheet-meta-quest-3/

[29] A. Michel, R. Colella, G. A. Casula, P. Nepa, L. Catarinucci, G. Montisci, G. Mazzarella, and G. Manara. 2018. Design Considerations on the Placement of a Wearable UHF-RFID PIFA on a Compact Ground Plane. *IEEE Transactions on Antennas and Propagation* 66, 6 (June 2018), 3142–3147. https://doi.org/10.1109/TAP.2018.2811863

[30] ST Microelectronics. 2017. IIS2MDC - High accuracy, ultralow-power, 3-axis digital output magnetometer - STMicroelectronics. https://www.st.com/en/mems-and-sensors/iis2mdc.html

[31] ST Microelectronics. 2020. VL53L1 - Time-of-Flight (ToF) long-distance ranging sensor with advanced multizone and multiobject detection - STMicroelectronics. https://www.st.com/en/imaging-and-photonics-solutions/vl53l1.html

[32] Noor Mohammed, Rui Wang, Robert W. Jackson, Yeonsik Noh, Jeremy Gummeson, and Sunghoon Ivan Lee. 2021. ShaZam: Charge-Free Wearable Devices via Intra-Body Power Transfer from Everyday Objects. *Proceedings of the ACM on Interactive, Mobile, Wearable and Ubiquitous Technologies* 5, 2 (June 2021), 1–25. https://doi.org/10.1145/3463505

[33] Rafael Morales González, Asier Marzo, Euan Freeman, William Frier, and Orestis Georgiou. 2021. UltraPower: Powering Tangible & Wearable Devices with Focused Ultrasound. In *Proceedings of the Fifteenth International Conference on Tangible, Embedded, and Embodied Interaction*. ACM, Salzburg Austria, 1–13. https://doi.org/10.1145/3430524.3440620

[34] Ezekiel Darlington Nwalike, Khalifa Aliyu Ibrahim, Fergus Crawley, Qing Qin, Patrick Luk, and Zhenhua Luo. 2023. Harnessing Energy for Wearables: A Review of Radio Frequency Energy Harvesting Technologies. *Energies* 16, 15 (Jan. 2023), 5711. https://doi.org/10.3390/en16155711 Number: 15 Publisher: Multidisciplinary Digital Publishing Institute.

[35] Powercast. 2013. P2110B 915MHz RF Powerharvester® Receiver. https://www.mouser.com/powercast-p2110-powerharvester

[36] Powercast. 2020. Transmitters. https://www.powercastco.com/transmitters/

[37] Vaishnavi Ranganathan, Sidhant Gupta, Jonathan Lester, Joshua R. Smith, and Desney Tan. 2018. RF Bandaid: A Fully-Analog and Passive Wireless Interface for Wearable Sensors. *Proceedings of the ACM on Interactive, Mobile, Wearable and Ubiquitous Technologies* 2, 2 (July 2018), 1–21. https://doi.org/10.1145/3214282

[38] Rishi Shukla, Neev Kiran, Rui Wang, Jeremy Gummeson, and Sunghoon Ivan Lee. 2019. SkinnyPower: enabling batteryless wearable sensors via intra-body power transfer. In *Proceedings of the 17th Conference on Embedded Networked Sensor Systems*. ACM, New York New York, 68–82. https://doi.org/10.1145/3356250.3360034

[39] Neeta Singh, Taimoor Khan, Sachin Kumar, Binod Kumar Kanaujia, Hyun Chul Choi, Kang Wook Kim, Karumudi Rambabu, Sembiam R. Rengarajan, and Ahmed A. Kishk. 2024. Ultra-thin flexible rectenna integrated with power management unit for wireless power harvester/charging of smartwatch/wristband. *Scientific Reports* 14, 1 (March 2024), 7447. https://doi.org/10.1038/s41598-024-57639-1 Publisher: Nature Publishing Group.

[40] Joshua R. Smith, Alanson P. Sample, Pauline S. Powledge, Sumit Roy, and Alexander Mamishev. 2006. A Wirelessly-Powered Platform for Sensing and Computation. In *UbiComp 2006: Ubiquitous Computing*, David Hutchison, Takeo Kanade,

Josef Kittler, Jon M. Kleinberg, Friedemann Mattern, John C. Mitchell, Moni Naor, Oscar Nierstrasz, C. Pandu Rangan, Bernhard Steffen, Madhu Sudan, Demetri Terzopoulos, Dough Tygar, Moshe Y. Vardi, Gerhard Weikum, Paul Dourish, and Adrian Friday (Eds.). Vol. 4206. Springer Berlin Heidelberg, Berlin, Heidelberg, 495–506. https://doi.org/10.1007/11853565_29 Series Title: Lecture Notes in Computer Science.

[41] Seeed Studio. 2023. Seeed Studio XIAO nRF52840 - Supports Arduino / CircuitPython- Bluetooth5.0 with Onboard Antenna. https://www.seeedstudio.com/Seeed-XIAO-BLE-nRF52840-p-5201.html

[42] Yuning Su, Yuhua Jin, Zhengqing Wang, Yonghao Shi, Da-Yuan Huang, Teng Han, and Xing-Dong Yang. 2023. Laser-Powered Vibrotactile Rendering. *Proceedings of the ACM on Interactive, Mobile, Wearable and Ubiquitous Technologies* 7, 4 (Dec. 2023), 1–25. https://doi.org/10.1145/3631449

[43] Ryo Takahashi, Masaaki Fukumoto, Changyo Han, Takuya Sasatani, Yoshiaki Narusue, and Yoshihiro Kawahara. 2020. TelemetRing: A Batteryless and Wireless Ring-shaped Keyboard using Passive Inductive Telemetry. In *Proceedings of the 33rd Annual ACM Symposium on User Interface Software and Technology*. ACM, Virtual Event USA, 1161–1168. https://doi.org/10.1145/3379337.3415873

[44] Ryo Takahashi, Eric Whitmire, Roger Boldu, Shiu Ng, Wolf Kienzle, and Hrvoje Benko. 2024. picoRing: battery-free rings for subtle thumb-to-index input. In *Proceedings of the 37th Annual ACM Symposium on User Interface Software and Technology*. ACM, Pittsburgh PA USA, 1–11. https://doi.org/10.1145/3654777.3676365

[45] Ryo Takahashi, Wakako Yukita, Tomoyuki Yokota, Takao Someya, and Yoshihiro Kawahara. 2022. Meander Coil++: A Body-scale Wireless Power Transmission Using Safe-to-body and Energy-efficient Transmitter Coil. In *CHI Conference on Human Factors in Computing Systems*. ACM, New Orleans LA USA, 1–12. https://doi.org/10.1145/3491102.3502119

[46] Shan-Yuan Teng, K. D. Wu, Jacqueline Chen, and Pedro Lopes. 2022. Prolonging VR Haptic Experiences by Harvesting Kinetic Energy from the User. In *Proceedings of the 35th Annual ACM Symposium on User Interface Software and Technology*. ACM, Bend OR USA, 1–18. https://doi.org/10.1145/3526113.3545635

[47] Le-Giang Tran, Hyouk-Kyu Cha, and Woo-Tae Park. 2019. A compact wireless power transfer system at 915MHz with supercapacitor for optogenetics applications. *Sensors and Actuators A: Physical* 285 (Jan. 2019), 386–394. https://doi.org/10.1016/j.sna.2018.11.029

[48] Hoang Truong, Shuo Zhang, Ufuk Muncuk, Phuc Nguyen, Nam Bui, Anh Nguyen, Qin Lv, Kaushik Chowdhury, Thang Dinh, and Tam Vu. 2018. CapBand: Battery-free Successive Capacitance Sensing Wristband for Hand Gesture Recognition. In *Proceedings of the 16th ACM Conference on Embedded Networked Sensor Systems*. ACM, Shenzhen China, 54–67. https://doi.org/10.1145/3274783.3274854

[49] Hubregt J. Visser, Shady Keyrouz, Amanuel Kihshen, and Irina Paraschiv. 2012. Optimizing RF energy transport: Channel modelling and transmit antenna and rectenna design. In *2012 Loughborough Antennas & Propagation Conference (LAPC)*. 1–8. https://doi.org/10.1109/LAPC.2012.6402945

[50] Dieff Vital, Shubhendu Bhardwaj, and John L. Volakis. 2020. Textile-Based Large Area RF-Power Harvesting System for Wearable Applications. *IEEE Transactions on Antennas and Propagation* 68, 3 (March 2020), 2323–2331. https://doi.org/10.1109/TAP.2019.2948521

[51] Vybronics. 2020. VLV041235L - 240hz Rectagular LRA Linear Vibration Motor. https://www.vybronics.com/linear-lra-vibration-motors/v-lv041235l Section: LRA Linear Resonant Actuator Vibration Motors.

[52] Paul Worgan and Mike Fraser. 2017. CoilMove: An Actuated to-body Energy Transfer System. In *Proceedings of the 2017 Conference on Designing Interactive Systems*. ACM, Edinburgh United Kingdom, 791–795. https://doi.org/10.1145/3064663.3064693

[53] Longhan Xie and Mingjing Cai. 2014. Human Motion: Sustainable Power for Wearable Electronics. *IEEE Pervasive Computing* 13, 4 (Oct. 2014), 42–49. https://doi.org/10.1109/MPRV.2014.67

[54] Xiaoying Yang, Jacob Sayono, Jess Xu, and Yang Zhang. 2024. Interaction-Power Stations: Turning Environments into Ubiquitous Power Stations for Charging Wearables. In *Extended Abstracts of the CHI Conference on Human Factors in Computing Systems*. ACM, Honolulu HI USA, 1–8. https://doi.org/10.1145/3613905.3650769

[55] Tengxiang Zhang, Xin Yi, Chun Yu, Yuntao Wang, Nicholas Becker, and Yuanchun Shi. 2017. TouchPower: Interaction-based Power Transfer for Power-as-needed Devices. *Proceedings of the ACM on Interactive, Mobile, Wearable and Ubiquitous Technologies* 1, 3 (Sept. 2017), 1–20. https://doi.org/10.1145/3130986